Published in final edited form as:
Brain Res. 2008 January 10; 1188: 76–86. doi:10.1016/j.brainres.2007.10.081.

Communication call evoked gamma-band activity in the auditory cortex of awake bats is modified by complex acoustic features

Andrei V. Medvedev and **Jagmeet S. Kanwal**
Dept. of Physiology and Biophysics, Georgetown University, 3900 Reservoir Rd, NW, Washington D.C., 20057

Abstract

Mustached bats emit an acoustically rich variety of calls for social communication. In the posterior primary auditory cortex, activity of neural ensembles measured as local field potentials (LFPs) can uniquely encode each call type. Here, we report that LFPs recorded in response to calls contain oscillatory activity in the gamma-band frequency range (>20 Hz). The power spectrum of these high frequency oscillations shows either two peaks of energy (at 40 Hz and 100 Hz), or just one peak at 40 Hz. The relative power of gamma-band activity in the power spectrum of a call-evoked LFP correlates significantly with the 'harmonic complexity' of a call. Gamma-band activity is attenuated with reversal of frequency modulated calls. Amplitude modulation, even when asymmetric across call reversals, has no significant effect on gamma-band activity. These results provide the first experimental evidence that complex features within different groups of species-specific calls modify the power spectrum of evoked gamma-band activity.

Classification terms

Speech; music; gamma-band oscillations; synchrony; temporal coding; population coding; binding; hearing; auditory processing; sensory and motor systems

1. Introduction

Neural encoding of spectro-temporal information for recognition of complex acoustic signals, such as speech sounds, is not well understood. One approach to tackling this complex problem is to study the neural responses simultaneously at the single cell and population levels. At the population level, synchronous oscillations provide a powerful mechanism to integrate activity within a local population of neurons as well as across long range, functionally connected neural structures (König et al., 1995). High frequency gamma-band oscillation driven temporal coordination of activity at the surface of the auditory cortex was previously described in response to tonal clicks and amplitude-modulated sounds (Barth and MacDonald, 1996; Brosch et al., 2002; Franowicz and Barth, 1995; MacDonald and Barth, 1995). These studies were based on epidural recordings in lightly anesthetized rats. The term "gamma-band" traditionally referred to high frequency activity that is 30 to 80 Hz. More recently, Crone and co-workers

Corresponding author and address for reprint requests: Jagmeet S. Kanwal, Dept. of Physiology and Biophysics, Georgetown University Medical Center, 3900 Reservoir Rd, NW, Washington, D.C., 20057-1460; Ph.: (202)-687-1305; Fax: (202)-687-0617; kanwalj@georgetown.edu.

have extended the upper limit of gamma band activity to ~150 Hz based on subdural electrocorticographic recordings in humans and define oscillation activity >70 Hz as "high gamma" (Sinai et al., 2005). Although a few recent studies implicate the role of gamma-band oscillations on speech sound perception in humans (Crone et al., 2001; Sinai et al., 2005), there is no information nor any direct evidence for their role in processing social or communication calls in animals.

Mustached bats use a number of call types for social interactions and have proven to be useful animal models for understanding the neural coding of complex acoustic signals both for echolocation and communication. A previous study showed that the temporal response pattern of neuronal ensembles and possibly single neurons in the posterior region of the primary auditory cortex (AIp) in mustached bats changes consistently for each call type and could carry sufficient information to uniquely encode each call type (Medvedev and Kanwal, 2004). Both, slow-wave, local field potentials (LFPs) and spiking activity at any locus within AIp was patterned after call-specific dynamics. This dynamic activity contributed to a distributed representation of 14 different call types. This mechanism of neural encoding is in contrast to the 'combination-sensitivity' (nonlinear facilitation of neural responses to combinations of sound features) that is rampant in other auditory cortical areas of mustached bats and is also present in many other vertebrate species (Fuzessery and Feng, 1983; Margoliash and Fortune, 1992; Ohlemiller et al., 1996; Rauschecker and Tian, 2004; Suga et al., 1978). The primary auditory cortex (AIp) of mustached bats contains a representation of the frequencies (from 7 kHz to 50 kHz) that are present in the fundamental of all communication calls emitted by this species (Kanwal et al., 1994).

Here we performed a spectral analysis on some of the same and newly acquired LFP and spiking data to examine the contribution of oscillatory activity in the neural coding of social calls. We recorded single unit activity and event-related LFPs simultaneously and at the same locus in response to the presentation of 7 frequency-shifted variants each for 14 different types of simple syllabic calls. LFPs were used to examine the presence of gamma-band activity (this study) in response to different simple syllabic call types that constitute a large part of the vocal repertoire of mustached bats (Kanwal et al., 1994). The major question we address in this study is whether LFPs contain stimulus-specific oscillatory activity. If so, what role does this activity play in the representation of calls? Can a component of this type of synchronous activity be detected within simultaneously recorded single unit activity at the same locus?

Our results suggest that a majority of species-specific calls presented to awake bats trigger "gamma-band" (20–100 Hz), activity within local field potentials (LFPs) recorded from the AIp area. The activity range that we observe from intracortical recordings overlaps the so called "low" and "high" gamma band activity as well as high beta (20–30 kHz) as classified by others. We refer to the range of frequencies 20 to 100 Hz, studied in our experiments, as simply "gamma-band activity". This frequency range appears to be a more natural and continuous range for the effects observed in mustached bats. We further show that the pattern of the power spectrum of evoked gamma-band activity present within LFPs can be used to classify different call types into at least three distinct groups. These patterns of neural activity could provide a basis for a perceptual classification of different call types. Single and/or few unit spiking activity, although generally too sparse to visibly show gamma band oscillations, is significantly correlated with the LFP data. These results provide the first experimental data for a proposed role of stimulus-locked gamma-band activity in a "call recognition event" within a neural network (Hopfield and Brody, 2000; Hopfield and Brody, 2001). As discussed, call recognition may be achieved via oscillatory activity within a local population of neurons that leads to perceptual grouping of acoustic features within a complex sound.

2. Results

2.1. Gamma-band components within LFP and spiking activity

Single and few-unit activity as well as LFPs were recorded from nearly 100 recording sites in the AIp area of seven bats. A total of 98 call variants were presented to awake bats when recording from each locus. LFPs to all call types can be obtained at any recording site within the AIp of mustached bats (Medvedev and Kanwal, 2004). Different call types are uniquely encoded by the spectrotemporal patterns of responses within AIp. This can be observed by conducting an MDS analysis of both call types and LFP/MUA activity (see Medvedev and Kanwal, 2004). A consistent classification of various call types based on the temporal pattern of the LFP is observed at different recording locations within AIp. The spectral components within an LFP waveform can be divided into a low (<20 Hz) and a high (>20 Hz) frequency range. A spectral analysis of the call-evoked LFPs revealed a significant bias for the presence of gamma-band frequency components (Figs. 1a to 1d).

In most locations, single and/or few unit spiking activity was too sparse to provide visible evidence of gamma band activity within the PSTH of the neuronal response. Poststimulus time histogram (PSTH) of the summed activity of two simultaneously recorded single units correlated with the gamma-band rhythm suggesting a phase locking to both positive and negative peaks of gamma-band oscillations within the LFP (Fig. 1e, f). This represented the best example for which spiking activity corresponding to gamma band oscillations is visibly obvious in a PSTH. To further analyze a relationship between evoked gamma-band responses and stimulus-locked spiking activity, we calculated correlations between poststimulus histograms of single and/or few units and the corresponding gamma-band response recorded from the same location, the latter being calculated as LFP filtered within 20–100 Hz. For each PSTH and LFP, a correlation function was calculated and its maximal absolute value was taken as a correlation index between PSTH and LFP. The correlation index was significantly positive (0.15 ± 0.005; mean ± s.e.; $p < 0.001$) in 41 out of 114 units (36%) and significantly negative (-0.17 ± 0.006; $p < 0.001$) in 73 units (64%). Positive or negative values of the correlation index corresponded to spiking (preferential firing) at positive or negative peaks of a gamma-band oscillation cycle, respectively.

In some cases, the observed gamma-band activity can be a component of a nonspecific broadband evoked response (for discussion, see Galambos 1992). To test for the independence of stimulus-locked gamma-band activity (>20 Hz) from the overall LFP response in our experiments, we analyzed statistical power distributions of the spectral estimates of evoked activity for each frequency 1, 2, 3,…, 100 Hz. We reasoned that if gamma-band activity is a component independent from lower frequencies within LFP, the gamma-band power and the low frequency power should change from trial to trial statistically independently from each other. Their trial-to-trial independence can be checked mathematically by calculating empirical power distributions over all trials for each frequency and compare those distributions pair-wise statistically. If for any two frequencies (e.g., 10 Hz and 40 Hz) power distributions are statistically different from each other, this would rule out the possibility that those two frequencies come from the same (broadband) process because the presence of at least two processes with different power distributions would be ascertained. This analysis performed for each call independently, revealed significant differences between the spectral distributions of the LFP at low and high frequencies (compare Fig. 2a to the control data in Fig. 2b, see also Fig. 2c). This provided statistical evidence that the gamma-band activity is not part of a broadband complex signal, but a neurophysiological response that is relatively independent from the low frequencies (<20 Hz) within the LFP response. We therefore suggest that evoked gamma-band activity may carry important information about the stimulus, which is obscured within the overall waveform of the event-related LFP by the low frequency components that

usually have amplitudes higher than that of oscillations within the gamma-band frequency range (see Fig. 1a,b).

2.2. Relationship between gamma-band component of LFP and acoustic structure

Our previous analysis showed that a close correspondence exists between a multidimensional scaled (MDS) representation of the waveforms of call-evoked LFPs and an MDS representation of the acoustic structure of calls themselves (Medvedev and Kanwal, 2004). The MDS representation of calls was based on a pair-wise correlation between the corresponding waveforms of the call-evoked LFPs. The MDS configuration revealed that the pattern of LFPs recorded in response to different call types contained sufficient systematic variation to discriminate between call types. As a result, the two-dimensional MDS plot provided a representation of the different call types such that there was a one-to-one correspondence between a call type and its LFP obtained in the AIp area. Regression analysis of each call parameter with the corresponding value of the x-coordinate in this LFP classification scheme showed the highest correlation with the pitch of the call. The value on the y-coordinate showed the highest correlation with the harmonic structure of different call types. In particular, the position of a call-evoked LFP along this axis (y-coordinate on the MDS plane) was significantly correlated with the 'harmonic complexity' of the corresponding call, which was quantified through calculation of the 'effective' frequency (f_{eff}). The 'effective' frequency was calculated as an 'average' frequency within the normalized power spectrum of that call, $f_{eff} = \Sigma f_n s(f_n)/\Sigma s(f_n)$, where $f_n = f/f_{max}$ is normalized frequency and $s(fn)$ is normalized spectrum (Medvedev and Kanwal, 2004).

The central part within the square box in figure 3a is a plot of the MDS configuration of calls published earlier (Medvedev and Kanwal, 2004). Instead of using the overall temporal structure of LFPs, here we examine the contribution of gamma-band frequencies to this classification scheme. Calls with a large number of harmonics within their spectra ('harmonic stack') and calls with broadband spectra (FM calls and 'noise-burst' calls) had a higher f_{eff} due to contribution of the high harmonics, i.e., a high-frequency spectral 'tail' and are placed in the upper part of Fig. 3a. To visualize the variations in the gamma-band component in the distribution of the LFPs in the MDS configuration, we placed the gamma-band waveforms obtained from high-pass filtered and averaged LFP responses to each call type around the perimeter of the MDS plot. We observed that the amplitude and spectrum of gamma-band activity for different call types varied according to call type. We analyzed the dependence of gamma-band components within the LFPs on both coordinates of the MDS scheme. The relative power of gamma-band activity in the spectrum of a call-evoked LFP did not correlate with the pitch/formant frequency (x-coordinate), but correlated significantly with the 'effective' frequency (Fig. 3b). To classify calls according to differences in the spectrum of gamma-band activity, we grouped LFPs categorically according to their position on the vertical axis (second factor of the MDS scheme or y-coordinate in the MDS plot). Grouping of LFPs into three distinct groups along the vertical axis proved to be the most meaningful. We averaged gamma-band waveforms of call spectra within each group to arrive at an average representation of the gamma-band spectrum for each group. This classification scheme captured three distinct patterns of gamma-band activity within LFPs. Group-averaged LFPs and their power spectra are shown in Fig. 3c and 3d, respectively. Spectra of calls in the first and the second groups had distinct peaks at gamma-band frequencies either at 40 or both at 40 and 100 Hz, whereas the third group lacked significant levels of gamma-band activity (Fig. 3d). We therefore propose that gamma-band activity components within call-evoked LFPs can be used to segregate call types into the following three groups: 1) 'harmonically rich' calls with a high number of harmonics (calls 1, 12, 6, 10, 11 in the top row of Fig. 3a); 2) calls with a low number of harmonics but relatively broad spectral peaks ('intermediate' group of calls 8, 9 with strong

FM and 'noise-burst' call 14) and, finally, 3) 'harmonically simple' calls with a low number of harmonics and weak FM (calls 5, 13, 7, 3 in the lower part of Fig. 3a).

2.3. Effect of call reversal on gamma-band activity

To test for the contribution of acoustic features within a call to the power of gamma-band activity, we examined whether call reversal modifies the pattern of call-evoked gamma-band activity within LFPs. We discovered that the overall temporal pattern of the LFP changed insignificantly with call reversal. Examples of averaged responses to two different call types are shown in figure 4a. In contrast, the gamma-band component within the same LFPs was attenuated by varying degrees when the animal was presented with reversed versions of the same call types (Fig. 4b). Figure 4c shows this result as a scatter plot of the power of gamma-band activity for forward (natural) versus reversed calls for all recorded locations tested for the majority of call types. Each data point is color-coded to match the three categories of gamma-band waveforms classified based on the MDS scheme (see fig. 3). Gamma-band activity in each category showed a similar scatter with points both above and below the diagonal. If gamma-band activity were the same for both straight and reversed calls, the corresponding points in the scatter plot would be placed on or close to the diagonal. The overall distribution of points in all three categories, however, showed a bias towards being above the diagonal suggesting that for many call types, gamma-band activity declined with call reversal. This means that call reversal leads to a redistribution of spectral power within the LFP significantly decreasing power at gamma frequencies (paired t-test, $p < 0.001$).

It is quite obvious that for a call reversal to have any physiological effect, that call should be asymmetric in time, i.e., change acoustically with reversal, because when the reversed copy of a call is acoustically similar to the original call, it is unlikely to produce any difference in the evoked response. This reasoning helps us explain why the gamma response changes with reversal of some calls and does not change with reversal of other calls. We should expect that those calls reversal of which evokes a change in gamma response should be more asymmetric in time. To test this effect statistically, we needed to have a quantitative measure of call symmetry in time as well as a quantitative measure of the change in gamma power with call reversal. The effect of call reversal can be characterized by the temporal symmetry in either its amplitude modulation (AM) and/or its frequency modulation (FM). AM of a call is usually characterized by its amplitude envelope while FM is characterized by a spectrogram. With call reversal, both the amplitude envelope and the spectrogram are also reversed. Then the similarity between the original envelope (or spectrogram) and its reversed copy can be measured by their correlation coefficient. Because correlation coefficient depends on mutual alignment of two signals and varies when one signal is shifted in respect to another, the perfect alignment should be sought which would give a highest correlation between two signals. To get highest correlation, the *correlation function* should be calculated, which gives correlation coefficients between two signals for all possible time shifts between them. The peak value of the correlation function will then provide the highest correlation coefficient between two signals. We therefore quantified the AM symmetry in time for each call type by calculating the maximum peak of a correlation function for the envelopes of a natural call and its reversed version. Similarly, we quantified the FM symmetry in time, by extracting the time waveform of the formant frequency modulation from the call spectrogram and measuring the maximum peak of the correlation function between the natural FM waveform and its reversed copy. Maximal correlations between 1) the original envelope and its reversed copy and 2) the original FM waveform and its reversed copy were taken as indexes of the AM and FM symmetry of a call, respectively.

To quantitatively assess the attenuation of gamma-band activity due to call reversal, we calculated a ratio of the response spectrum to a reversed call divided by the response spectrum to a natural call. This ratio was integrated over the gamma-band 20–100 Hz resulting in a

"reversed-to-natural-call gamma-band" (RNCG) ratio. A lower RNCG ratio indicated a greater attenuation of the mean response to a particular call type with reversal. The values of RNCG ratios were plotted against the 'AM symmetry' and the 'FM symmetry' indexes of the corresponding call. The AM symmetry index had no significant effect on the level of gamma-band activity (regression line slope = 0.16 ± 0.53 (mean ± s.d.) and insignificantly different from 0 at $p = 0.76$, $n = 14$; Fig. 5a). For calls with a lower 'FM symmetry' index, gamma-band activity was significantly (by 10% to 40%) attenuated with call reversal showing significant correlation with the FM symmetry index (Fig. 5b). Calls with increasing FM symmetry, e.g., call types 3, 8, 9, 10 and 12, showed a lower attenuation (higher RNCG ratio) compared to those with a lower FM symmetry, e.g., call types 6 and 7. The RNCG ratio significantly correlates with the FM symmetry index (regression line slope = 0.67 ± 0.16 (mean ± s.d.) and significantly >0 at $p = 0.0017$, Pearson's correlation coefficient $r = 0.8$; $n = 12$). Thus, the gamma-band response, but not the classical evoked potential (LFP), showed sensitivity to the natural spectro-temporal structure of communication calls. This provides neurophysiological evidence that the stimulus-locked gamma-band activity is an independent process within broadband evoked activity. Furthermore, call reversal has systematic effects on gamma-band activity depending on the level of FM symmetry present within a particular call type. Call types that are classified as constant frequency or CF calls (#s 1, 2 and 3) are spectrally more symmetrical than those containing steep FM components. Clearly, FM symmetry is not the only criterion determining the level of attenuation of gamma-band activity with call reversal. For some calls with high FM symmetry, the RNCG ratio showed a significantly greater variance compared to calls with low FM symmetry (strong FM modulation) (Fig. 5c). This suggests that other factors, such as AM modulation and rise-time of sound onset may influence the neural responses to some call types, e.g., #s 3 and 8, that show high levels of FM symmetry, so that the value of the RNCG ratio is highly variable across recording locations (Fig. 5c). Highly asymmetrical calls types, e.g,, #s 6 and 7, gave a more consistent result (a smaller standard deviation of the RNCG ratio) over all locations tested. The noisy calls, 13 and 14, were excluded from this analysis since they lack clear FM components.

3. Discussion

Gamma-band oscillations were previously observed within olfactory and visual systems (Desmedt and Tomberg, 1994; Eckhorn et al., 1988; Engel et al., 1992; Fiser et al., 2004; Gevins et al., 1994; Gray and Singer, 1989; Ikegaya et al., 2004; Lam et al., 2003; Martin et al., 2004; Nikonov et al., 2002; Pulvermuller, 1996; Ribary et al., 1991; Sannita et al., 2001; Tiesinga and Sejnowski, 2004). In a few cases, gamma-band oscillations have also been observed in relation to motor behaviors (Donoghue et al., 1998; Maynard et al., 1999). Keyser and Konig (Kayser and Konig, 2004) reported stimulus locking to 23–39 Hz and 109 Hz frequency bands in addition to lower frequencies within LFPs in V1. Evoked gamma-band activity was first described in the auditory modality as a transient phase-locked response within 60–100 ms poststimulus (Galambos, 1992; Pantev et al., 1991). Recently, gamma band oscillations (~35 Hz) together with those in the theta (~7 Hz) and low delta (~1.3 Hz) range have also been implicated in cross-modal interactions, particularly between the somatosensory and auditory systems (Lakatos et al., 2007). Regardless, the role of fast oscillations in perceptual grouping remains controversial (Tovee and Rolls, 1992), and only a few studies have addressed its functional role (Crone et al., 2001; Karakas and Basar, 1998; Knief et al., 2000).

The data presented in this study provide evidence for a role of gamma-band activity within local field potentials for the perception of communication calls. Preliminary data suggest that this is also reflected to some extent in the single to few-unit spiking activity, although this is less robust due to the sparseness of spiking in auditory cortical neurons. Single unit data on peak firing rates obtained in the cortex of marmosets (Liang et al., 2002) substantiates our

difficulty of finding single unit activity that showed firing rates in the range of gamma band activity, although, there is significant phase-locking to frequencies in the gamma band range. The high frequency (>20 Hz) oscillatory activity appears to reflect the level of harmonic complexity within a call and may be triggered by the convergence of multiple and harmonically related frequency inputs to a neuron. This is consistent with the harmonic tuning of the majority of AIp neurons in the mustached bat's auditory cortex. Below we discuss our results in support of inter-related roles of gamma band activity in population coding, perceptual grouping and in call recognition.

3.1. Population coding and gamma-band activity

Representation of information in the brain involves the activities of either sparse or large numbers of neurons. Therefore the concept of population coding is central to an understanding of information processing and representation of calls in the auditory cortex. Population coding assumes that highly specialized neurons are neither necessary nor sufficient to encode complex stimuli, such as calls. In this context, oscillation of neural activity in the gamma band can play an important role in coordinating the simultaneous activation of local populations of neurons.

Our peak firing rate data in the AIp area show that neurons here are not highly specialized and respond to multiple call stimuli. That is, they do not exhibit combination-sensitivity as in other areas of the auditory cortex. However, they do exhibit different temporal patterns in the averaged single unit activity as well as in LFP recordings (Medvedev and Kanwal, 2004). Studies of the mammalian central auditory system, especially in echolocating bats, have revealed that temporal codes are intricately related to and implemented as population codes (Covey, 2000). Our call response data in the AIp area are consistent with this hypothesis. Although the evidence for and against a time structure in neural activity in the mammalian cortex is mixed, the existing data nevertheless suggest that the cerebral cortex is capable of preserving fine timing information (Cariani, 1999). This may be done via a firing rate code of combination-sensitive neurons that are phase-locked to a stimulus (O'Neill and Suga, 1982; Suga et al., 1979) or in the firing pattern of neuronal ensembles that is the outcome of synaptic inputs and spiking activity of a small population of neurons (Victor and Conte, 2000).

A population code may consist of a common, stimulus-driven statistical structure of the population activity. Alternatively, it may use temporal relationships between members of a neural population to represent information. Gamma-band oscillations may emerge from the latter mechanism of encoding information within a population. A temporal population code may include interdependence (synchrony, correlation or coherence) of the activity of individual neurons in a population. This is labeled as 'coordinated-coding' (deCharms and Zador, 2000) or 'ensemble-coding' (Cariani, 1999). Changes in coordinated firing in the absence of changes in firing rate have been found in the primary auditory, frontal and motor cortices (Abeles et al., 1993; deCharms and Merzenich, 1996; Hatsopoulos et al., 1998; Prut et al., 1998). In a recent review of the literature on gamma-band oscillations and their neuronal mechanisms, it has been suggested that pyramidal neurons that are strongly activated, fire with high discharge rates early in the gamma cycle. This provides a computational mechanism for the implementation of a temporal coding scheme that enables fast processing and flexible routing of activity (Fries et al., 2007). This mechanism relies on the conversion of amplitude to phase and is based more on coincident detection than on rate integration. Our finding of a significant level of correlation between single unit activity and gamma-band oscillations within the LFP is consistent with this suggestion. Neurons are more likely to discharge at times close to the peaks of oscillations and the relative timing of the neuronal discharge within the oscillatory cycle may facilitate in the transmission of a temporally coded "information wave". Both, the timing and contents of this packet of information may have important consequences for perception.

An important question to consider with respect to the role of oscillatory activity in neural coding has to do with what the specific stimulus parameters that are being encoded. Clearly, amplitude and frequency modulations are two important parameters that others have examined using synthetic stimuli where these parameters can be quantified and systematically manipulated. In their study on awake marmosets, Liang et al. (2002) found that 60% of the recorded units showed statistically significant discharge synchrony to sinusoidal amplitude and frequency modulated (sAM and sFM, respectively) stimuli and the population averaged mean firing rate peaked at 16 to 32 Hz.

An analysis of the spectral content of bat vocalizations suggests that frequency modulations within narrow bands of frequencies in the majority of call types are not necessarily correlated with the AM of the narrow band or the overall AM of the call (Kanwal et al., 1994; Medvedev and Kanwal 2004). This is not surprising given the fact that for frequencies in the ultrasonic range, the recorded AM of a call can be influenced by the head aim of the emitter and the relative location of the microphone. It should also be noted that some calls are shorter than the duration of even one gamma cycle and therefore cannot have amplitude or frequency modulations at gamma-band frequencies. For example, call #1 with duration of less than 10 ms, which evoked a strong gamma-band activity in the LFP. Furthermore, calls consisting of constant and quasi-constant frequencies also trigger neural activity in the gamma band so that gamma oscillations in the neural activity cannot be solely attributed to the sAM or sFM in a stimulus. Therefore, one of the conclusions from this study is that high frequency oscillations (20–100 Hz) within the LFP are not a simple reflection of modulations within sounds (a resonance-like phenomenon) but rather a population-level mechanism which, being sensitive to the spectro-temporal structure of calls, may be involved in coding of complex acoustic parameters of sounds and call recognition.

3.2. Role of gamma-band activity in perceptual grouping

Oscillatory activity may play a key role in perceptual grouping i.e., temporal binding of feature elements (Malsburg, 1981; Malsburg, 1986; Milner, 1974). According to this hypothesis, oscillations contribute to temporal binding of the independent variables within a complex stimulus. Highly correlated and phase-locked activity in several locations underlies the gestalt of a cohesive and coherent object (Crick, 1984; Malsburg, 1986). The dynamics of correlative activity has been shown to pose some temporal limitations which make oscillations in the gamma-band range 20–100 Hz within a small population of neurons a most suitable “carrier” to reliably and rapidly express correlated neural activty (König and Schillen, 1991).

Our results provide a critical link between auditory processing for communication in animals and humans and also suggest that gamma-band activity signifies a common multineuron mechanism for processing and/or perception of stimuli in all sensory modalities.

For the auditory system, there is some evidence that an evoked gamma-band response depends on the complexity of the auditory task (Karakas and Basar, 1998). Using a ‘virtual pitch’ paradigm, i.e., a complex auditory stimulus with a missing fundamental, Knief and colleagues demonstrated functional differences of evoked gamma-band activity due to the perception of coherent versus non-coherent auditory stimuli in humans (Knief et al., 2000). Comparing MEG responses to speech versus non-speech sounds, Palva et al. have suggested that evoked gamma-band activity may be sensitive to high-level stimulus properties and may reflect the natural representation of speech sounds (Palva et al., 2002). The presence of gamma-band activity in response to species-specific communication sounds in a nonprimate mammalian species suggests that this mechanism may be parsimonious, especially in species that employ a rich variety of call types for auditory communication.

3.3. Role of gamma-band activity in call recognition

In the auditory modality, some controversy exists regarding the independence of evoked gamma-band activity from the broadband 'classical' evoked potential (Galambos, 1992; Medvedev and Kanwal, 2004; Pantev et al., 1991). Narrow-band filtering can artificially create oscillatory components within neural activity (Bertrand and Tallon-Baudry, 2000). If evoked activity represents a unitary process with a broadband spectrum, all its spectral components should have the same power distribution determined by the statistical properties of the underlying process. If, however, evoked activity is not uniform, it may incorporate a number of individual processes or components with different statistical and spectral properties. The power distributions of those components are likely to be different.

In our experimental data, we observed that evoked gamma-band activity in the 20–100 Hz range is statistically independent from the major low frequency components (<20 Hz) in the evoked LFP. This conclusion is based on two results. First, power distributions at gamma-band frequencies differ significantly from power distributions at low frequencies in the LFPs. Second, gamma-band oscillation, but not the gross evoked potential, shows a significant correlation with the spectrotemporal structure of calls (Fig. 4). Calls with a complex harmonic structure, i.e., calls with a strong FM and calls with a high number of harmonics, evoke a stronger gamma-band activity compared to calls with a simpler spectral structure. A possible interpretation of this finding is that a complex harmonic structure requires integration over a larger set of "feature elements" encoding specific spectral parameters of sounds. An enhanced evoked gamma-band oscillation may thus indicate synchrony of neuronal elements within larger cortical networks where the integrative processes related to sound representation and recognition take place. Also, the evoked gamma-band activity is attenuated with time reversal of calls, which have a strong temporal asymmetry in their spectral components, such as calls that contain a strong upward or downward FM. The strength of the evoked gamma-band activity may be correlated to call familiarity and may therefore act as a "recognition" mechanism. Accordingly, calls corrupted by time reversal evoke a significantly weaker gamma-band response because they are not 'recognized'.

Hopfield and Brody have proposed that a 'call recognition event' occurs when transient synchronization of neuronal firing patterns is achieved through the temporal convergence of synaptic currents within a subset of neurons that are activated by the call (Hopfield and Brody, 2000; Hopfield and Brody, 2001). This transient synchrony of neuronal firing is accompanied by the appearance of gamma-band oscillations within the activity of a population of neurons. According to this model, the population transient synchrony is extremely sensitive to the specific temporal structure of a sound and is achieved through facilitation of synaptic connections within the neural population when the sound is learnt and becomes familiar. Time reversal of a familiar sound changes its temporal structure and, as a result, transient population synchrony is not achieved, the gamma-band response is absent and the sound is not recognized. Our results on the sensitivity of the gamma-band response to time reversal of calls are consistent with the predictions of this model and provide the first experimental data confirming that stimulus-locked gamma-band activity may be either a signature or an outcome of a "call recognition event" within a neural network. Furthermore, our data show that in the mustached bat, reversals of FM are more important that that of AM. For some call types, the large variation in the change in gamma-band activity for forward versus reversed call types suggests that gamma-band activity is likely influenced by additional parameters, such as AM modulations and rise time of sound onset and their interaction with sound duration (Kaiser et al., 2007) as well as recording location. In humans, learning of temporally modulated tone trains increases the power of high (62–98 Hz) gamma band activity in the inferior frontal cortex and is a potential neural substrate for top-down modulation of learning-induced plasticity in the auditory cortex (van Wassenhove and Nagarajan, 2007). Multisite, single and multiunit

recordings *in-vivo* together with *in-vitro* studies of synaptic physiology can further substantiate the neural mechanisms underlying gamma band oscillations in the neocortex (Cunningham et al., 2004).

4. Experimental Procedures

The surgery, acoustic stimulation methods and recording of electrophysiological activity for these experiments are similar to those described previously (Kanwal et al., 1999) and are only briefly described here.

4.1. Surgery and Recording of Neural Activity

During electrophysiological recordings from mustached bats, *Pteronotus parnellii*, the head of the bat was restrained by clamping the metal post glued to the surface of the skull and the bat's body was suspended in a Styrofoam mold by elastic bands in a heated (31 C), sound proofed and echo-attenuated chamber (IAC 400A) monitored with a video camera. The electrophysiological activity was recorded with vinyl-coated tungsten microelectrodes with tip diameters of ~10 μm and impedance of ~1 MΩ inserted into the cortex perpendicular to the skull to a depth of 300–600 μm through a small (50 μm) hole. The amplified signal was band-pass filtered between 600 Hz and 4 kHz for recording of neuronal action potentials and LFPs were recorded from the same electrode with a low band-pass filter (1–300 Hz) and sampling frequency of 1024 Hz. All surgeries and animal experiments were performed with approval of the Georgetown University Animal Care and Use Committee.

4.2. Acoustic stimuli

CF tone bursts were used to identify the best frequency (BF) and "call-scans" were performed to identify the best call (BC) at each recording site. The best frequency and the best call were defined as stimuli evoking the largest response of the single unit (the largest peak in the PSTH). Tones were presented from two condenser loudspeakers mounted on a vertical hoop and positioned 95 cm directly in front of the bat. The two loudspeakers were positioned adjacent to each other in the same azimuth in front of the bat to avoid binaural effects. The stimulus generation and delivery system consisted of three channels, two analog and one digital. The three sounds could be independently controlled in frequency, amplitude and duration and could be delivered simultaneously or successively. These sounds could be triggered either manually or via a computer. The condenser loudspeakers were calibrated by placing a B & K microphone at the position of the ear and were reasonably flat between 20 and 100 kHz with a significant roll off at 120 kHz. The maximum amplitude level that could be delivered for speaker A was 98 dB SPL (re 20 μPa, RMS) at 90 kHz and that for speaker B was 95 dB SPL at 85 kHz.

Sound stimuli used in this study were 30 ms long CF tones with a 1 ms rise and fall time and simple syllabic calls of the same species that were digitized at a 250 kHz sample rate and/or synthesized using the SIGNAL software (Engineering Design Inc.). The values of BFs and the approximate harmonic relationship between the BFs were used to distinguish AIp neurons from DSCF neurons which are tuned to a pair of non-harmonic frequencies (Kanwal et al., 1999).

To deliver the natural calls and their variants (ranging in duration from 4 ms to 89 ms) at a rate of 1/s, another computer (Pentium PC) with an A/D-D/A board (DT 2821G) and a sound generation program SIGNAL were used. The main set of fourteen call types consisted of calls averaged over the population of bats (Kanwal et al., 1994). Calls were assigned numbers from 1 to 14 based on their acoustic classification via multidimensional scaling (Kanwal et al., 1994). A pseudorandom sequence of presentation of call types did not change either the relative or absolute response magnitude of calls when presented at a rate of 1 per second. During the first phase of the call scans, a 15-second epoch of neural activity (no stimulus control plus

fourteen different types of simple syllabic calls presented at a rate of one call per second) was recorded. After every ten consecutive presentations at the same level of loudness, the sound intensity of each call was automatically decreased by 25 dB. Thus, three levels of intensity (95, 70 and 45 dB on average) were tested initially over a total of 30 trials. This three-step intensity screening was done using all seven sets of calls (the 'standard' call and its six variants with spectra shifted by ±1, ±2 and ±3 standard deviations of a call's fundamental frequency). The data from this initial screening were analyzed on-line to reveal the best call-variant for each call type. At the second stage of the screening process, a newly configured set of the best variants for each of the fourteen call types was presented at six different intensity levels (from ~100 to ~50 dB SPL with attenuation steps of 10 dB). As a result of the two-step screening procedure, call preference was determined for every recording site in exactly the same manner. Frequency variants of these "standard" calls were synthesized on the computer by shifting the spectrum of the mean waveform up and down by 1 to 3 standard deviations of the call main frequency as measured across the bat population (Kanwal et al., 1994). In most cases, mean waveforms represent an average of several hundred examples of each call type obtained from either a colony or a small group of bats.

4.3. Data Analysis

The best call was determined on the basis of peak firing rates for single and/or few-unit activity at each recording locus. The best variants of each call type were then presented at five different intensity levels (90 to 50 dB SPL) to identity the best call types among the best variants and its best amplitude for excitation. These 2 or 3 calls were then presented 200 times to obtain an averaged, representative LFP for each call type. The response of 3 to 5 best or "preferred" call variants was recorded for 50 to 100 presentations at their optimal level of sound intensity. Background activity was also recorded for 1 second before each repetition of the auditory stimulus set. Each call was also presented to the animal in the reverse order and the corresponding LFPs as well as single- or few unit responses were recorded. In total, 138 cortical sites in the left hemisphere of 6 bats were studied.

Peri-stimulus time histograms (PSTH's) and LFPs were calculated for 200 presentations of acoustic stimuli at the rate of 1/s and with a 5 ms pre-stimulus time and bin width of 1 ms. LFP power spectra were calculated using Welch's periodogram method based on fast Fourier transformation (FFT) with Hanning window. Evoked gamma-band oscillations were extracted by filtering the LFP between 20–100 Hz. To obtain the empirical power distributions of evoked activity, we first calculated a sample power spectrum of electrical activity for each of 200 single trials. Power values were then normalized to have a zero mean value and a standard deviation equal to one over all single trials. Thus, 200 sample z-transformed values of spectral power were obtained and used to calculate an empirical distribution of those values at each frequency 1, 2, 3,…, 100 Hz. Those normalized distributions were then compared pair-wise for every two frequencies using Smirnov's criterion to test the null-hypothesis that those distributions are not significantly different at a significance level of $p=0.01$.

To analyze acoustic parameters of calls, we calculated the 'effective' frequency which reflects harmonic structure of a call (Medvedev and Kanwal, 2004) as well as two parameters characterizing spectrotemporal structure of a call, namely, FM and AM symmetry indexes. To calculate the AM symmetry index, we first extracted an amplitude envelope for each call and its reversed version. We then calculated correlation function for the envelopes of a natural call and its reversed version. Correlation function is a function of time and reflects a similarity of two signals at different temporal shifts between them. Its absolute value may take values between 1 (when signals are identical) and 0 (when signals are not related to each other). The maximum peak of correlation function between the envelopes of a natural call and its reversed version was taken as an AM symmetry index. Similarly, for the FM symmetry index, we first

calculated the formant frequency of a call at every time point from the call time-frequency spectrogram, which gave us the time course, or 'waveform', of changes in formant frequency in time. The maximum peak of correlation function between the 'formant frequency waveform' of a natural call and its reversed version was taken as an FM symmetry index.

Acknowledgments

We thank the Ministry of Agriculture, Land and Marine Resources in Trinidad for permitting us to export mustached bats, and F. Muradali who assisted with the collection and exportation procedures. This research was supported by National Institute on Deafness and other Communication Disorders (NIH Grant R01 DC02054 to JSK).

Literature References

Abeles M, Bergman H, Margalit E, Vaadia E. Spatiotemporal firing patterns in the frontal cortex of behaving monkeys. J Neurophysiol 1993;70:1629–38. [PubMed: 8283219]

Barth DS, MacDonald KD. Thalamic modulation of high-frequency oscillating potentials in auditory cortex. Nature 1996;383:78–81. [PubMed: 8779725]

Bertrand O, Tallon-Baudry C. Oscillatory gamma activity in humans: a possible role for object representation. Int J Psychophysiol 2000;38:211–23. [PubMed: 11102663]

Brosch M, Budinger E, Scheich H. Stimulus-related gamma oscillations in primate auditory cortex. J Neurophysiol 2002;87:2715–25. [PubMed: 12037173]

Cariani P. Temporal coding of periodicity pitch in the auditory system: an overview. Neural Plast 1999;6:147–172. [PubMed: 10714267]

Covey E. Neural population coding and auditory temporal pattern analysis. Physiol Behav 2000;69:211–220. [PubMed: 10854931]

Crick F. Function of the thalamic reticular complex: the searchlight hypothesis. Proc Natl Acad Sci USA 1984;81:4586–4590. [PubMed: 6589612]

Crone NE, Boatman D, Gordon B, Hao L. Induced electrocorticographic gamma activity during auditory perception. Brazier Award-winning article, 2001. Clin Neurophysiol 2001;112:565–82. [PubMed: 11275528]

Cunningham MO, Whittington MA, Bibbig A, Roopun A, LeBeau FE, Vogt A, Monyer H, Buhl EH, Traub RD. A role for fast rhythmic bursting neurons in cortical gamma oscillations in vitro. Proc Natl Acad Sci U S A 2004;101:7152–7. [PubMed: 15103017]

deCharms RC, Merzenich MM. Primary cortical representation of sounds by the coordination of action-potential timing. Nature 1996;381:610–3. [PubMed: 8637597]

deCharms RC, Zador A. Neural representation and the cortical code. Annu Rev Neurosci 2000;23:613–47. [PubMed: 10845077]

Desmedt JE, Tomberg C. Transient phase-locking of 40 Hz electrical oscillations in prefrontal and parietal human cortex reflects the process of conscious somatic perception. Neurosci Lett 1994;168:126–129. [PubMed: 8028764]

Donoghue JP, Sanes JN, Hatsopoulos NG, Gaal G. Neural discharge and local field potential oscillations in primate motor cortex during voluntary movements. J Neurophysiol 1998;79:159–173. [PubMed: 9425187]

Eckhorn R, Bauer R, Jordan W, Brosch M, Kruse W, Munk M, Reitboeck HJ. Coherent oscillations: a mechanism of feature linking in the visual cortex? Multiple electrode and correlation analyses in the cat. Biol Cybern 1988;60:121–130. [PubMed: 3228555]

Engel AK, König P, Kreiter AK, Schillen TB, Singer W. Temporal coding in the visual cortex: new vistas on integration in the nervous system. Trends Neurosci 1992;15:218–226. [PubMed: 1378666]

Fiser J, Chiu C, Weliky M. Small modulation of ongoing cortical dynamics by sensory input during natural vision. Nature 2004;431:573–8. [PubMed: 15457262]

Franowicz MN, Barth DS. Comparison of evoked potentials and high-frequency (gamma-band) oscillating potentials in rat auditory cortex. J Neurophysiol 1995;74:96–112. [PubMed: 7472356]

Fries P, Nikolic D, Singer W. The gamma cycle. Trends Neurosci 2007;30:309–16. [PubMed: 17555828]

Fuzessery ZM, Feng AS. Mating call selectivity in the thalamus of the leopard frog, (Rana pipiens): single and multiunit analyses. J Comp Physiol 1983;150:333–344.

Galambos, R. A comparison of certain gamma band (40 Hz) brain rhythms in cat and man. In: Basar, E.; Bullock, TH., editors. Induced Rhythms in the Brain. Birkhauser; Boston, Basel, Berlin: 1992. p. 201-216.

Gevins A, Cutillo B, Desmond J, Ward M, Bressler S, Barbero N, Laxer K. Subdural grid recordings of distributed neocortical networks involved with somatosensory discrimination. Electroencephalogr Clin Neurophysiol 1994;92:282–290. [PubMed: 7517850]

Gray CM, Singer W. Stimulus-specific neuronal oscillations in orientation columns of cat visual cortex. Proc Natl Acad Sci USA 1989;86:1698–1702. [PubMed: 2922407]

Hatsopoulos NG, Ojakangas CL, Paninski L, Donoghue JP. Information about movement direction obtained from synchronous activity of motor cortical neurons. Proc Natl Acad Sci USA 1998;95:15706–15711. [PubMed: 9861034]

Hopfield JJ, Brody CD. What is a moment? “Cortical” sensory integration over a brief interval. Proc Natl Acad Sci U S A 2000;97:13919–24. [PubMed: 11095747]

Hopfield JJ, Brody CD. What is a moment? Transient synchrony as a collective mechanism for spatiotemporal integration. Proc Natl Acad Sci U S A 2001;98:1282–7. [PubMed: 11158631]

Ikegaya Y, Aaron G, Cossart R, Aronov D, Lampl I, Ferster D, Yuste R. Synfire chains and cortical songs: temporal modules of cortical activity. Science 2004;304:559–64. [PubMed: 15105494]

Kaiser J, Leiberg S, Rust H, Lutzenberger W. Prefrontal gamma-band activity distinguishes between sound durations. Brain Res. 2007

Kanwal JS, Fitzpatrick DC, Suga N. Facilitatory and inhibitory frequency tuning of combination-sensitive neurons in the primary auditory cortex of mustached bats. J Neurophysiol 1999;82:2327–2345. [PubMed: 10561409]

Kanwal JS, Matsumura S, Ohlemiller K, Suga N. Analysis of acoustic elements and syntax in communication sounds emitted by mustached bats. J Acoust Soc Am 1994;96:1229–1254. [PubMed: 7962992]

Karakas S, Basar E. Early gamma response is sensory in origin: a conclusion based on cross-comparison of results from multiple experimental paradigms. Int J Psychophysiol 1998;31:13–31. [PubMed: 9934618]

Kayser C, Konig P. Stimulus locking and feature selectivity prevail in complementary frequency ranges of V1 local field potentials. Eur J Neurosci 2004;19:485–9. [PubMed: 14725644]

Knief A, Schulte M, Bertran O, Pantev C. The perception of coherent and non-coherent auditory objects: a signature in gamma frequency band. Hear Res 2000;145:161–8. [PubMed: 10867289]

König P, Schillen TB. Stimulus-dependent assembly formation of oscillatory responses: I. Synchronisation. Neural Comput 1991;3:155–66.

König P, Engel AK, Singer W. Relation between oscillatory activity and long-range synchronization in cat visual cortex. Proc Natl Acad Sci U S A 1995;92:290–294. [PubMed: 7816836]

Lakatos P, Chen CM, O’Connell MN, Mills A, Schroeder CE. Neuronal Oscillations and Multisensory Interaction in Primary Auditory Cortex. Neuron 2007;53:279–292. [PubMed: 17224408]

Lam YW, Cohen LB, Zochowski MR. Odorant specificity of three oscillations and the DC signal in the turtle olfactory bulb. Eur J Neurosci 2003;17:436–46. [PubMed: 12581162]

Liang L, Lu T, Wang X. Neural representations of sinusoidal amplitude and frequency modulations in the primary auditory cortex of awake primates. J Neurophysiol 2002;87:2237–2261. [PubMed: 11976364]

MacDonald KD, Barth DS. High frequency (gamma-band) oscillating potentials in rat somatosensory and auditory cortex. Brain Res 1995;694:1–12. [PubMed: 8974632]

von der Malsburg, C. The correlation theory of brain function. Internal Report 81-2. Max-Planck-Inst. Biophys. Chem., Gottingen. In: Domany, E.; van Hemmen, JL.; Schulten, K., editors. Models of neural networks II. Temporal aspects of coding and information processing in biological systems. Springer-Verlag; N.Y: 1981. p. 95-119.1994

von der Malsburg, C. Am I thinking assemblies?. In: Palm, G.; Aertsen, A., editors. Brain Theory. Springer-Verlag; Berlin Heidelberg: 1986. p. 161-76.

Margoliash D, Fortune ES. Temporal and harmonic combination-sensitive neurons in the zebra finch's HVc. J Neurosci 1992:4309–4326. [PubMed: 1432096]

Martin C, Gervais R, Hugues E, Messaoudi B, Ravel N. Learning modulation of odor-induced oscillatory responses in the rat olfactory bulb: a correlate of odor recognition? J Neurosci 2004;24:389–97. [PubMed: 14724237]

Maynard EM, Hatsopoulos NG, Ojakangas CL, Acuna BD, Sanes JN, Normann RA, Donoghue JP. Neuronal interactions improve cortical population coding of movement direction. J Neurosci 1999;19:8083–8093. [PubMed: 10479708]

Medvedev AV, Kanwal JS. Local field potentials and spiking activity in the primary auditory cortex in response to social calls. J Neurophysiol 2004;92:52–65. [PubMed: 15212439]

Milner PM. A model for visual shape recognition. Psychol Rev 1974;81:521–535. [PubMed: 4445414]

Nikonov AA, Parker JM, Caprio J. Odorant-induced olfactory receptor neural oscillations and their modulation of olfactory bulbar responses in the channel catfish. J Neurosci 2002;22:2352–62. [PubMed: 11896174]

O'Neill WE, Suga N. Encoding of target range and its representation in the auditory cortex of the mustached bat. J Neurosci 1982;2:17–31. [PubMed: 7054393]

Ohlemiller KK, Kanwal JS, Suga N. Facilitative responses to species-specific calls in cortical FM-FM neurons of the mustached bat. Neuroreport 1996;7:1749–1755. [PubMed: 8905657]

Palva S, Palva JM, Shtyrov Y, Kujala T, Ilmoniemi RJ, Kaila K, Naatanen R. Distinct gamma-band evoked responses to speech and non-speech sounds in humans. J Neurosci 2002;22:RC211. [PubMed: 11844845]

Pantev C, Makeig S, Hoke M, Galambos R, Hampson S, Gallen C. Human auditory evoked gamma-band magnetic fields. Proc Natl Acad Sci U S A 1991;88:8996–9000. [PubMed: 1924362]

Peng JP, Medvedev AV, Kanwal JS. Multipeaked frequency tuning and responses to social calls in the posterior primary auditory cortex of mustached bats. (in revision)

Prut Y, Vaadia E, Bergman H, Haalman I, Slovin H, Abeles M. Spatiotemporal structure of cortical activity: properties and behavioral relevance. J Neurophysiol 1998;79:2857–74. [PubMed: 9636092]

Pulvermuller F. Hebb's concept of cell assemblies and the psychophysiology of word processing. Psychophysiology 1996;33:317–333. [PubMed: 8753932]

Rauschecker JP, Tian B. Processing of band-passed noise in the lateral auditory belt cortex of the rhesus monkey. J Neurophysiol 2004;91:2578–89. [PubMed: 15136602]

Ribary U, Ioannides AA, Singh KD, Hasson R, Bolton JP, Lado F, Mogilner A, Llinás R. Magnetic field tomography of coherent thalamocortical 40-Hz oscillations in humans. Proc Natl Acad Sci USA 1991;88:11037–11041. [PubMed: 1763020]

Sannita WG, Bandini F, Beelke M, De Carli F, Carozzo S, Gesino D, Mazzella L, Ogliastro C, Narici L. Time dynamics of stimulus- and event-related gamma band activity: contrast-VEPs and the visual P300 in man. Clin Neurophysiol 2001;112:2241–9. [PubMed: 11738194]

Sinai A, Bowers CW, Crainiceanu CM, Boatman D, Gordon B, Lesser RP, Lenz FA, Crone NE. Electrocorticographic high gamma activity versus electrical cortical stimulation mapping of naming. Brain 2005;128:1556–1570. [PubMed: 15817517]

Suga N, O'Neill WE, Manabe T. Cortical neurons sensitive to combinations of information-bearing elements of biosonar signals in the mustached bat. Science 1978;200:778–781. [PubMed: 644320]

Suga N, O'Neill WE, Manabe T. Harmonic-sensitive neurons in the auditory cortex of the mustached bat. Science 1979;203:270–274. [PubMed: 760193]

Tiesinga PH, Sejnowski TJ. Rapid temporal modulation of synchrony by competition in cortical interneuron networks. Neural Comput 2004;16:251–75. [PubMed: 15006096]

Tovee MJ, Rolls ET. Oscillatory activity is not evident in the primate temporal visual cortex with static stimuli. Neuroreport 1992;3:369–72. [PubMed: 1515598]

van Wassenhove V, Nagarajan SS. Auditory cortical plasticity in learning to discriminate modulation rate. J Neurosci 2007;27:2663–72. [PubMed: 17344404]

Victor JD, Conte MM. Two-frequency analysis of interactions elicited by Vernier stimuli. Vis Neurosci 2000;17:959–73. [PubMed: 11193112]

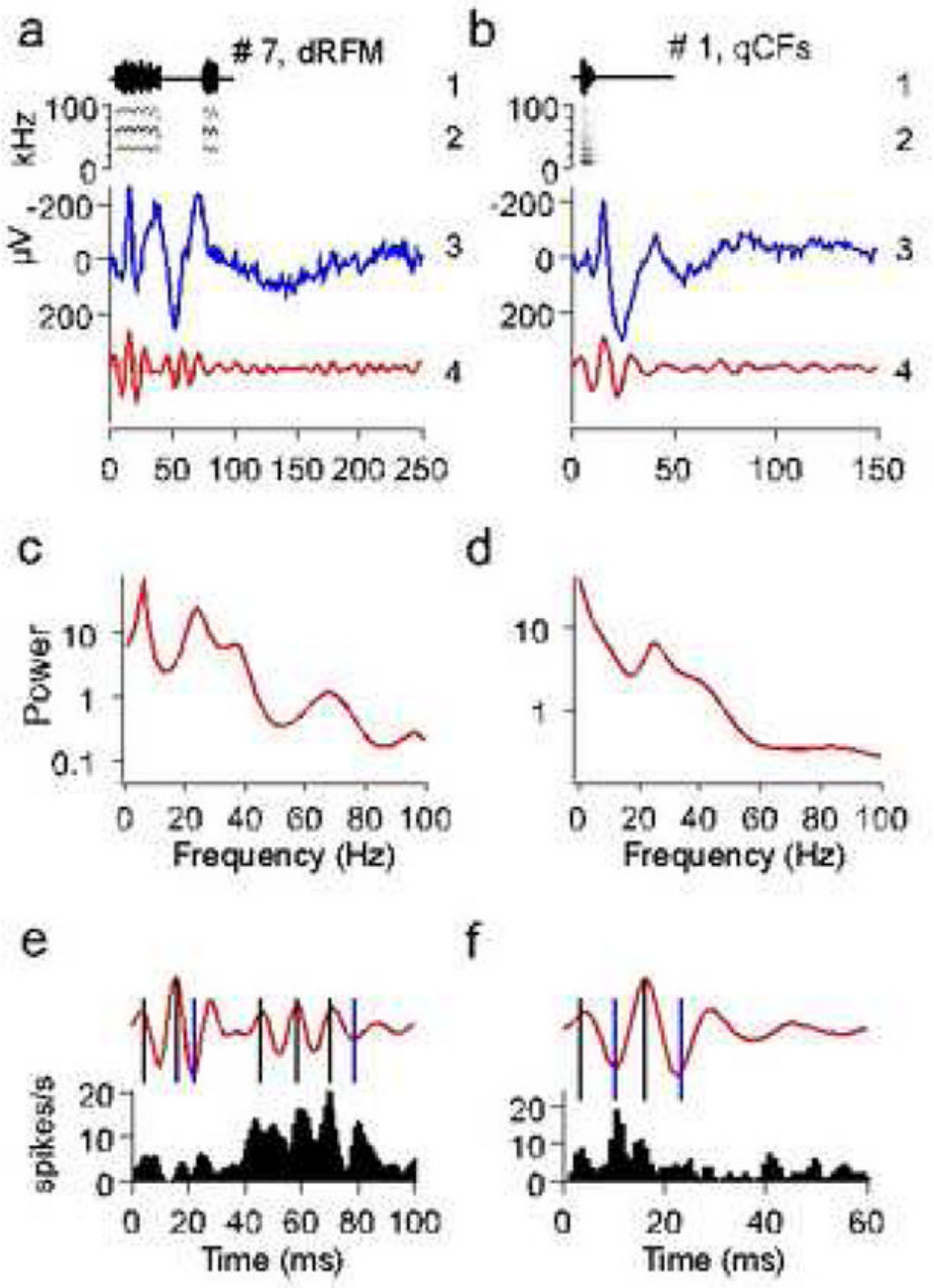

Fig. 1.

Communication calls, call-evoked local field potentials (LFP) and their power spectra. Bat communication signals consist of simple 'syllables', or monosyllabic calls (Kanwal et al., 1994). Two examples in (**a**) and (**b**) show calls # 7 (descending Rippled FM or dRFM) and # 1 (short quasi CF or qCFs), respectively, with call amplitude envelopes (1) and spectrograms (2) as well as the corresponding LFPs (3) and the 'gamma-band responses' obtained by band-pass filtering the LFP from 20–100 Hz (4). (**c**, **d**) Power spectra of the LFPs shown in (**a**) and (**b**), respectively. Note prominent spectral peaks at frequencies above 20 Hz. (**e**, **f**) Gamma-band responses shown in (a) and (b) are reproduced at a higher temporal resolution along with the corresponding PSTHs summed from two simultaneously recorded single units. Note that

peaks of neuronal activity coincide with either positive (marked by black vertical lines) or negative (marked by blue vertical lines) peaks of gamma-band oscillations.

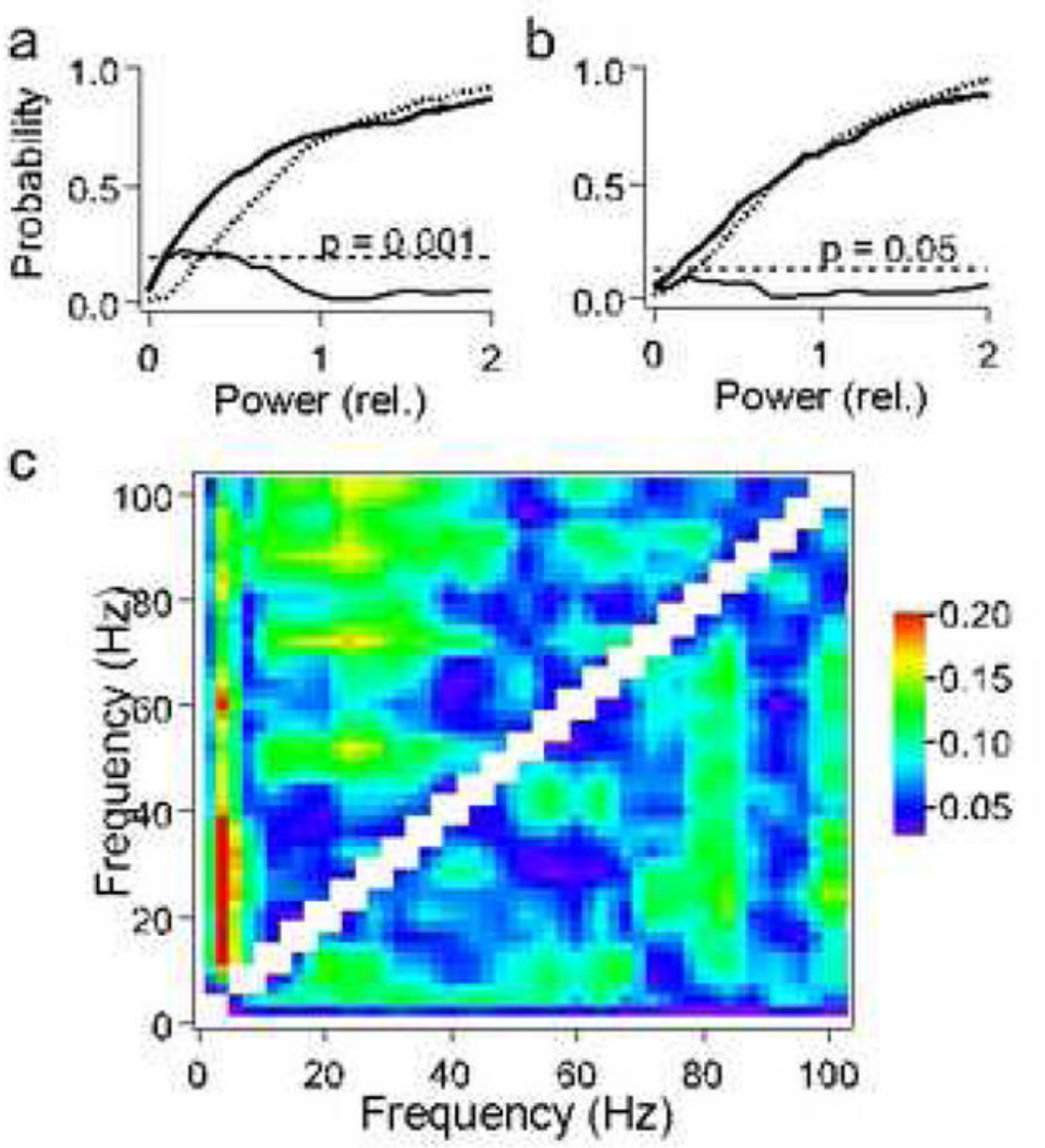

Fig. 2.

Empirical power distributions of the LFP spectra over 200 repetitions of the same call. The descending Rippled FM (dRFM) call shown in figure 1a is always emitted as a pair of syllables. The difference (thin line) between the empirical probability functions describing power distributions at frequencies 3 Hz (bold line) and 40 Hz (dotted line) is significant for the LFP ($p<0.001$)(**a**) and insignificant for the control data ($p>0.05$)(**b**) obtained by band-pass filtering 1–100 Hz of the Gaussian white noise (Smirnov's criterion). (**c**) Color matrix for maximal differences between the power distributions of the LFP spectrum for all pair-wise comparisons between frequencies 1, 2,…, 100 Hz for call 7 (upper left part of the matrix) and call 1 (lower right part of the matrix). These differences are significant (red color, $p<0.001$; green color,

$p<0.05$) for high frequencies (>20 Hz) versus low frequencies (<20 Hz). Note that there are also significant differences between power distributions within the range of beta-gamma-band frequencies. This may indicate that there are several sources and/or types of gamma-band oscillations at different frequencies, which are relatively independent of each other. For example, for call 7, gamma-band rhythms at 53 Hz, 72 Hz and 87 Hz may be independent from rhythms at 25 Hz, as indicated by regions of yellow and green colors.

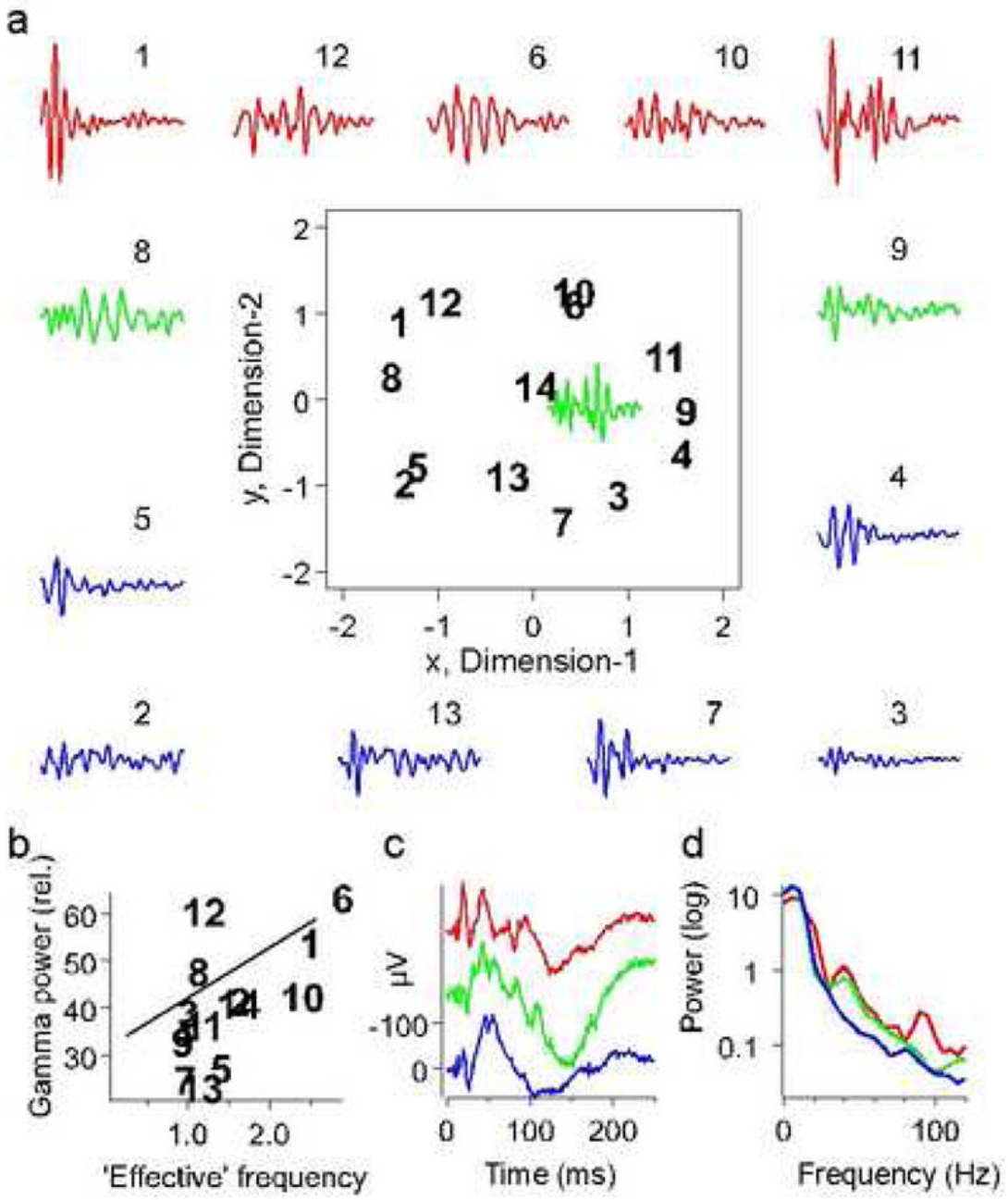

Fig. 3.

Effect of harmonic structure of calls on the evoked gamma-band response. (**a**) Gamma-band responses are placed along the perimeter of the two-dimensional scaling plot segregating calls according to their 'harmonic complexity' quantified by the 'effective' frequency of a call (Medvedev and Kanwal, 2004). Gamma-band responses to calls with a high number of harmonics (i.e., the 'effective' frequency is high) are shown in red, gamma-band responses to calls with a low number of harmonics but broadband spectra due to a strong FM (intermediate values of the 'effective' frequency) are shown in green and gamma-band responses to calls with a low number of harmonics and weak FM (the 'effective' frequency is low) are shown in blue. (**b**) The amount of gamma-band activity in the LFP power spectra normalized to their

average power over 1–100 Hz (‘relative’ spectra) significantly correlated with the ‘effective’ frequency of a call (regression line slope >0 at p=0.02). (**c**) Group-averaged LFPs. (**d**) Power spectra of the group-averaged LFPs. Note the prominent spectral peaks at gamma-band frequencies in the LFP spectra for groups 1 (red) and 2 (green).

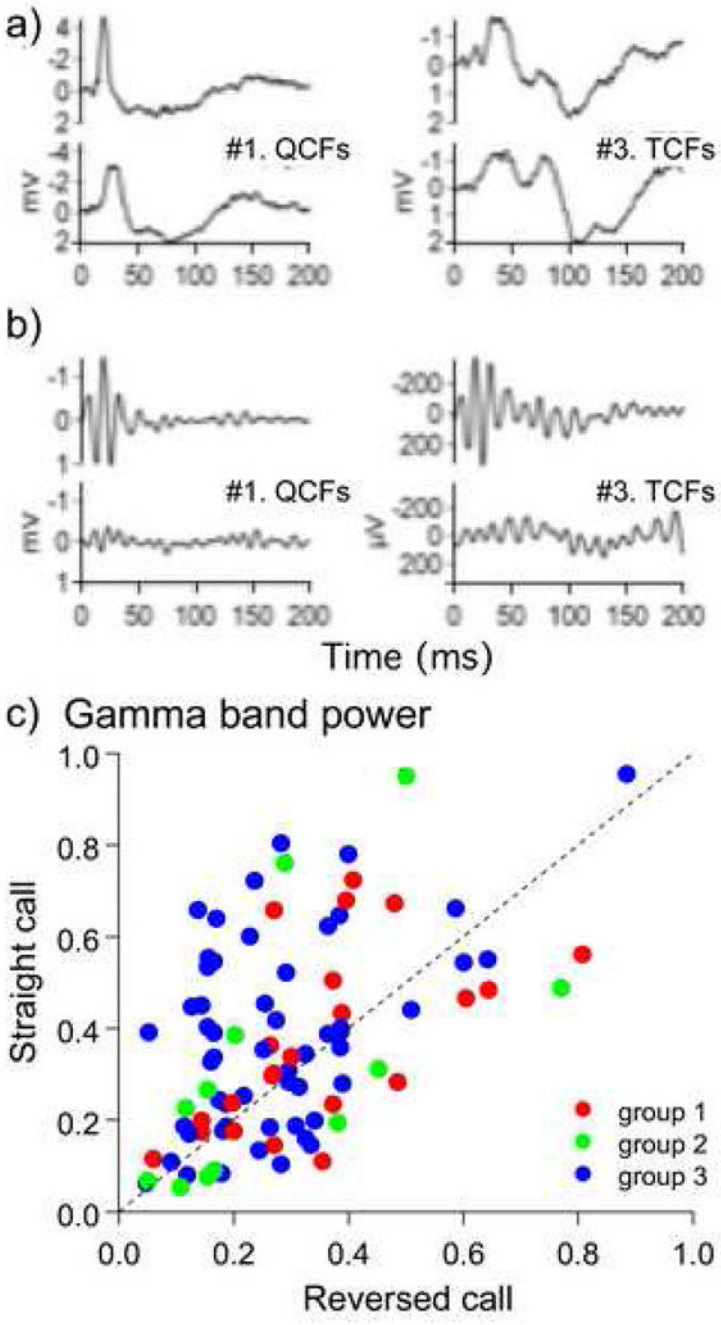

Fig 4.

LFPs (a) and evoked gamma-band activity within 20–100 Hz filtered from the LFP (b) during presentation of two natural calls (top traces) and the same calls reversed in time (bottom traces). Note that call reversal does not affect the waveform and the temporal profile of the slow components of the LFP (a) while the gamma-band response to reversed calls is attenuated (b). Scatter plot in (c) shows the effect of call reversal on gamma-band activity for each call type and for every recording site. For each call presented in the forward and the reverse direction, the corresponding LFP spectra are calculated and normalized to their average power to compensate gross amplitude changes. Gamma-band power is calculated by integrating the LFP spectra over the range 20–100 Hz. Power values for the straight calls 1–14 are plotted against

the corresponding values for the reversed calls. Note that the distribution of points within the scatter plot is not symmetrical and has a wider scattering, especially for group 3 (blue dots) above the bisector line; if call reversal did not change the spectral content of a LFP, the scatter plot would be symmetrical around the bisector line. Filled circles are colored according to their placement in the three groups along the y-axis of the MDS plot as shown in figure 3.

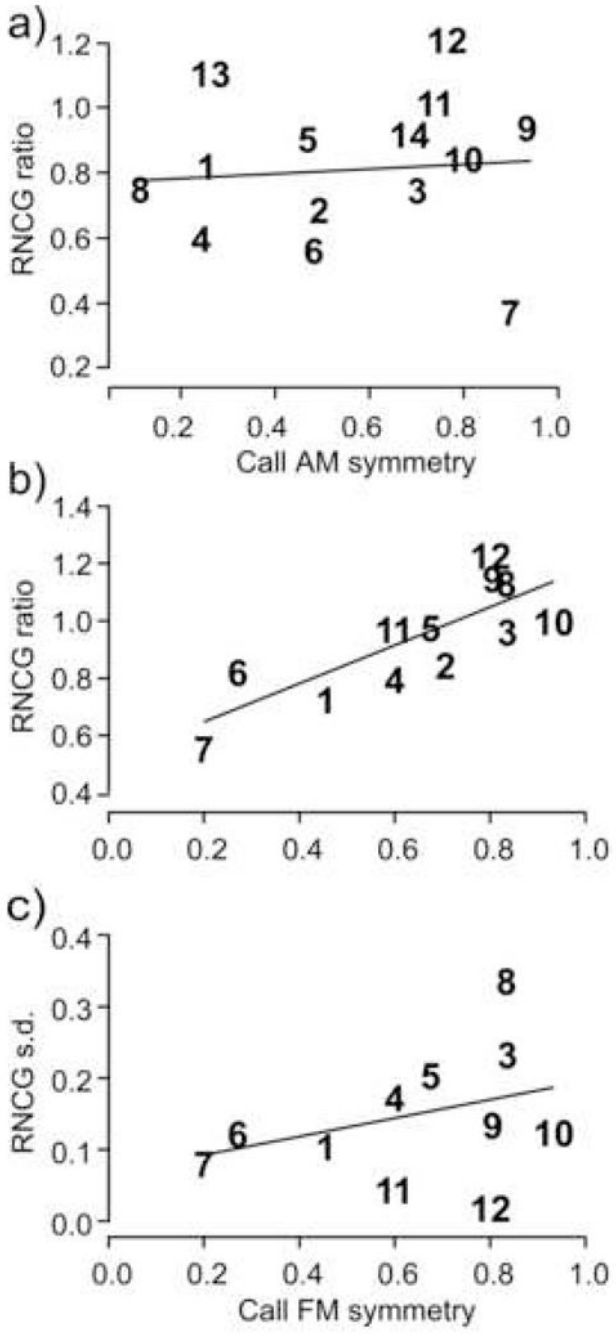

Fig. 5.

Gamma-band response to reversed calls: effect of (**a**) AM symmetry, and (**b**) FM symmetry of each call type. Reversed-to-Natural-Call Gamma-band (RNCG) ratio in (a) and (b) is calculated as a ratio of the averaged gamma-band response to the reversed call divided by the averaged gamma-band response to the natural call. This ratio versus the AM (a) and FM (b) symmetry indexes of all call types are plotted. For the AM symmetry, regression line slope = 0.16 ± 0.53 (mean ± s.d.) and is insignificantly different from 0 ($p = 0.76$, $n = 14$). Contrary to that, the RNCG ratio significantly correlates with the FM symmetry index (regression line slope = 0.67 ± 0.16 and significantly >0 at $p = 0.0017$, $n = 12$). c) Standard deviation (s.d.) of gamma-band power within LFP to a reversed call is plotted against the corresponding FM

symmetry index for each call type. Note a greater variability of gamma-band response for reversed calls with high FM symmetry within 0.6–1 range. The regression line (slope = 0.13 ± 0.12, mean ± s.d.) is insignificantly different from zero ($p = 0.3$; Pearson's correlation coefficient, $r = 0.34$; $n = 12$). Calls are assigned numbers from 1 to 14 based on their acoustic classification (Kanwal et al., 1994). FM symmetry was not calculated for call types 13 and 14 that are patterns of noise bursts.